

Proceeding of ICNM - 2009

1st International Conference on Nanostructured Materials and Nanocomposites (6 – 8 April 2009, Kottayam, India)

Published by : Applied Science Innovations Private Limited, India.

<http://www.applied-science-innovations.com>

Investigation of structural and optical properties of tin dioxide

Jagriti^a and Pratima Chuhan*

Physics Department, University of Allahabad, Allahabad-211002, India.

e mail :* nanomateriallab@gmail.com, mangul67@yahoo.co.in

Abstract : Tin dioxide nanoparticles were prepared using a cationic surfactant [Cetyltrimethyl ammonium Bromide: $\text{CH}_3(\text{CH}_2)_{15}\text{N}^+(\text{CH}_3)_3\text{Br}^-$] as the organic template and the hydrous tin chloride ($\text{SnCl}_4 \cdot 2\text{H}_2\text{O}$) and NH_4OH as the inorganic precursor. Analysis was performed by X-ray diffraction, TEM (Transmission electron microscopy), UV-Vis absorption, Photoluminescence and Raman spectroscopy. The XRD data of the as prepared sample shows the pattern are indexed to the rutile phase without any trace of an extra phase and particle size 7~8 nm which is further confirmed by TEM analysis. The UV-Vis spectra shows that the absorption edge is blue shifted and the band gap of the prepared sample is 4.0 eV which is larger than the bulk SnO_2 (3.6 eV).

Keywords : SnO_2 , Nanoparticles, CTAB

Introduction : With the growing interest in the building advance materials using nanoscale building blocks , the study for the fabrication of inorganic nanoparticles with controlled size and shape is continually being intensified. Nanostructure of oxide material are of considerable interest in the area of chemical sensing due to the improved sensitivity of nanostructures to the reducing gases compared to bulk oxide materials .The improved sensitivity of the nanostructured oxides are due to the availability of high surface area and grain boundary sites in the nanostructured oxides. Tin dioxide (SnO_2) is the most popular sensing material due to advantages such as low cost, high sensitivity and the ability to miniaturize and integrate on micromachined substrates. SnO_2 in its pure form is an n-type semiconductor with a direct band gap of 3.6 eV between the full oxygen 2p valence band and the tin states at the bottom of the conduction band. Because of its optical (transparent for visible light and reflective for IR) and the electrical properties, allied to good chemical and mechanical stability, it can be used in many application such as transparent conductive electrodes, photovoltaic devices, photo sensors, catalysis and antistatic coating. However, its most important use is as the active layer in the gas sensing devices¹⁻⁴ for which measurement of the electrical conductivity allows the concentration of inflammable and toxic gases(H_2 , CO , CH_4 ,.....) to be monitored.

Various methods have been reported to synthesize nanocrystalline SnO₂. In this paper we have approached a surfactant mediated method⁵. Because physical and chemical properties of nanomaterials do not depend only on the composition but also on the particle size a good synthesis protocol has to provide good control over particle size. The surfactant plays an important role in the controlled preparation of SnO₂ nanoparticles. The surfactant serves as micro reactors to confine the crystal growth. The properties of the materials were characterized by X-Ray diffraction (XRD) analysis, Transmission Electron Microscopy(TEM), Ultraviolet-Visible(UV), Photoluminescence (PL), Raman and Fourier Transform Infra Red (FTIR) spectroscopy.

Experimental Detail:

Sample preparation:

For preparing the sample we have used cetyl-tri ammonium bromide(CTAB), SnCl₄.2H₂O and liquor ammonia(MERCK). A homogeneous 0.08 M solution of CTAB was obtained by mixing the CTAB with double distilled deionized water. The solution of the diluted NH₃.H₂O (25 %) was added to the CTAB solution with continuous stirring. A 0.34 M solution of SnCl₄.2H₂O was added to the above homogeneous solution. After stirring at room temperature, the product was aged for two days. The resulting precipitates were filtered, followed by washing with distilled water to remove the excess CTAB. The sample was then dried at ambient temperature.

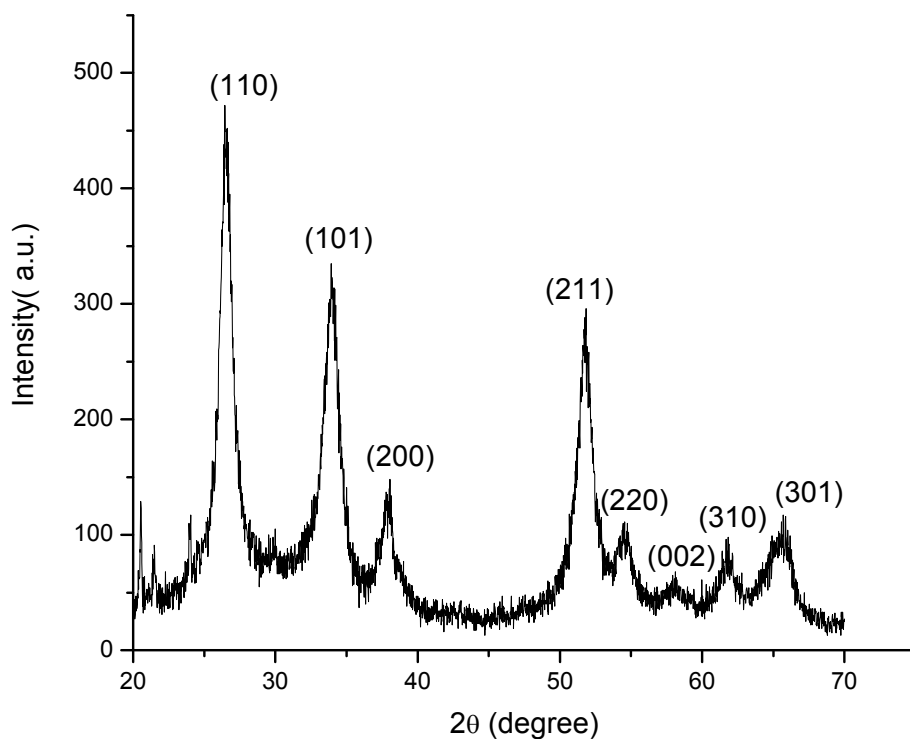


Fig. 1 XRD pattern for the prepared SnO₂ nanoparticles

Characterization techniques :

Rigaku D-max XRD with fixed Cu-K α line ($\lambda=1.54 \text{ \AA}$) was used for recording X-ray diffraction pattern operating at 30kV and 30 mA at steps 0.05° . Transmission Electron Microscopy (TEM) was performed by an electron microscope (Tecnai 20 G²) with an accelerating voltage of 200 kV. Samples for TEM were prepared by ultrasonically dispersing the product in ethanol, and the droplets were placed on carbon coated Cu grids. UV-Vis absorption spectra were recorded on Lambda 35 Perkin Elmer in the range 250-550 nm. LS 55 Perkin Elmer spectrophotometer was used for recording of photoluminescence of colloidal solution of SnO₂ NPs with 425nm and 450nm excitation lines. Raman spectrum was recorded at room temperature. The spectrum was excited by 488 nm line of an Ar⁺ laser in the backscattering configuration and recorded by using 0.5 M triple grating monochromator (Acton Research Corp. Spectra Pro, USA) coupled with PMT(R928, Hamamatsu) detector by using spectra sense software. The spectral resolution was 1 cm^{-1} . The dried SnO₂ nanoparticles were mixed with KBr, palletized and placed in the path of IR beam of GX Perkin Elmer Infrared spectrophotometer for the recording of FTIR spectrum.

Results and Discussion :

Fig.(1) shows the XRD pattern of as prepared samples. All the diffraction lines are assigned well to tetragonal rutile crystalline phase of tin oxide with a reference pattern (JCPDS 41-1445). The crystalline size (D) of the prepared powders was estimated using the Scherrer equation as follows -

$$D = \frac{0.9\lambda}{\beta \cos \theta}$$

Where λ , β and θ are the X-ray wavelength, the full width at half maximum (FWHM) of the diffraction peak and the Bragg diffraction angle respectively. Furthermore it is known that FWHM can be interpreted in terms of lattice strain and crystalline size which can be expressed by the following equation –

$$\frac{\beta \cos \theta}{\lambda} = \frac{1}{D} + \frac{\mu \sin \theta}{\lambda}$$

Where D and μ are the effective particle size and the effective strain. The effective particle size taking strain into account can be obtained by plotting $\beta \cos \theta / \lambda$ versus $\sin \theta / \lambda$. The particle size estimated by Debye Scherrer formula was 7~8 nm. We calculated the lattice parameters of the prepared sample as $a = 4.737 \text{ \AA}$, $c = 3.1611 \text{ \AA}$. When compared to bulk SnO₂ [$a=4.7382 \text{ \AA}$, $c=3.1871 \text{ \AA}$] there is a decrease in the c. This can be attributed to lattice strain which is calculated using $(\Delta c/c)$ to be 0.8%. We observe the almost equal values of lattice strain (0.6%) and effective particle size (9.2nm) by plotting $\beta \cos \theta / \lambda$ versus $\sin \theta / \lambda$.

Fig 2(a) shows the TEM image of the prepared tin dioxide nanoparticles. Particle size estimated by TEM micrographs are about 10 nm. Fig 2(b) presents the SAED pattern taken from the nanoparticles which can be indexed as a tetragonal rutile SnO₂^{6,7} in good

agreement with the XRD results and it shows that the as prepared samples have good crystallinity.

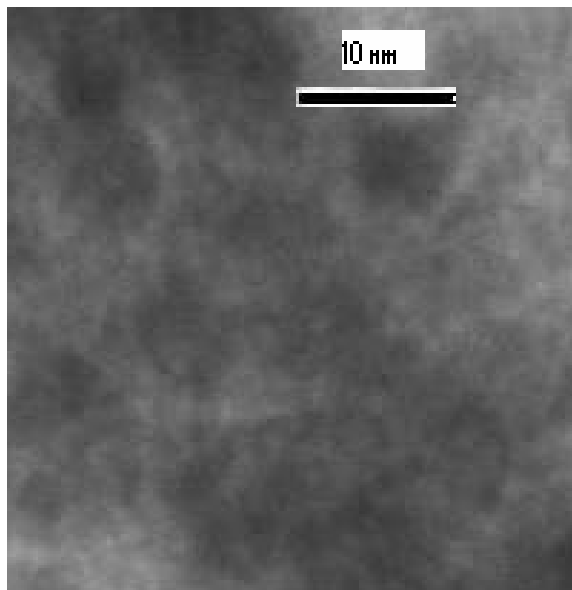


Fig. 2 (a) : TEM micrograph of SnO₂ nanoparticles.

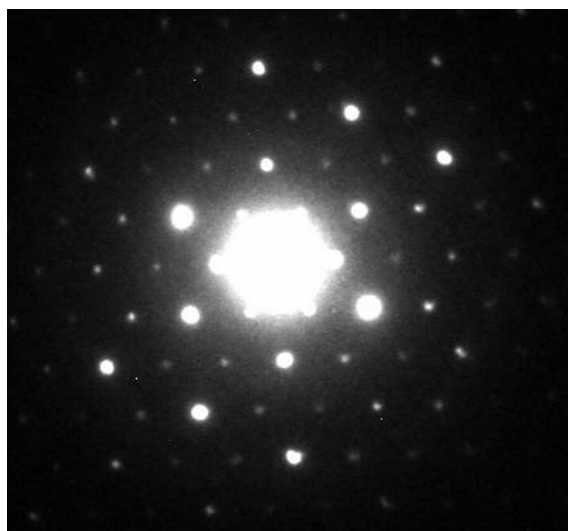


Fig.2 (b) : Electron Diffraction Pattern of SnO₂ nanoparticles.

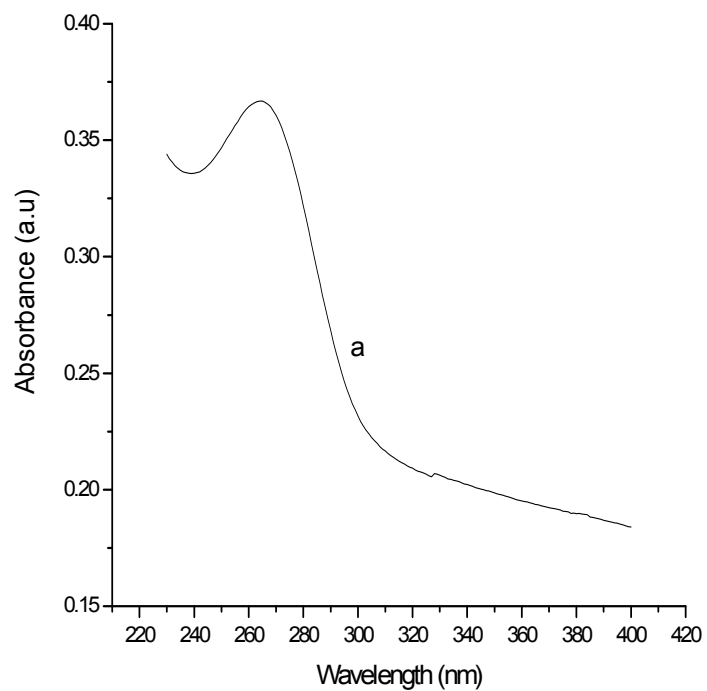


Fig. (3) : UV-Vis absorption spectrum of SnO₂ nanoparticles.

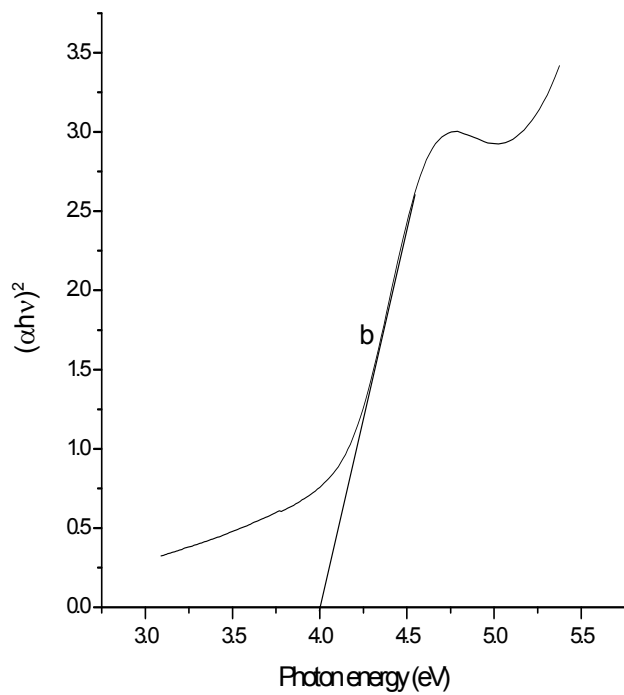


Fig .4 Plot of $(\alpha h\nu)^2$ versus $h\nu$ for as prepared SnO₂ nanoparticles.

The optical absorbance coefficient α of a semiconductor close to the band edge can be expressed by the following equation

$$\alpha = A (h\nu - E_g)^n / h\nu$$

where α is the absorption coefficient, E_g is the absorption band gap, A is constant, n depends on the nature of the transitions, n may have values $1/2$, 2 , $3/2$ and 3 corresponding to allowed direct, allowed indirect, forbidden direct and forbidden indirect transitions respectively. In this case $n=1/2$ for direct allowed transition. We evaluated effective band gap of prepared SnO_2 from the plot $(\alpha h\nu)^2$ vs. $h\nu$ fig.4. The band gap of the as prepared SnO_2 nanoparticles is 4.0 eV which is larger than the value of 3.6 eV for the bulk SnO_2 . This can be explained because bandgap of semiconductors have been found to be particle size dependent. The band gap increases with decreasing particle size and the absorption edge is shifted to a higher energy with decreasing particle size. The absorption spectrum of SnO_2 nanoparticles is shown in the fig.3 and the value of the absorption edge is 309 nm (about 4.0 eV). Considering the blue shift of the absorption position from the bulk SnO_2 , the absorption onset of the present sample can be assigned to the direct transition of electron in the SnO_2 nanocrystals⁸.

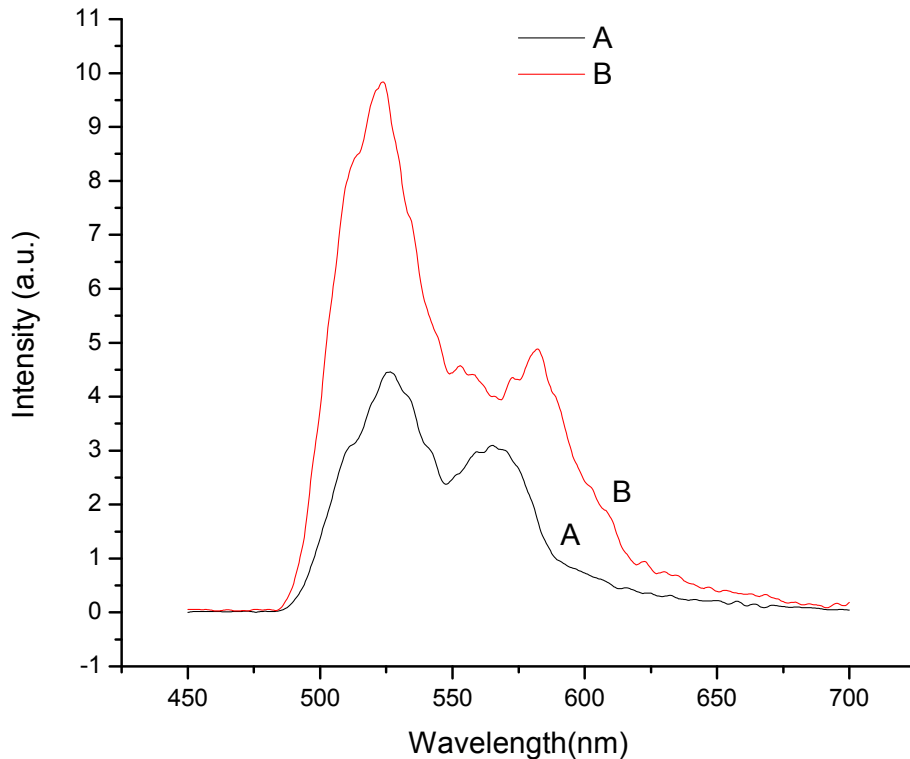


Fig. (5) : PL spectra of the SnO_2 nanoparticles at (A) $\lambda_{\text{ex}} = 425$ nm (B) $\lambda_{\text{ex}} = 450$.

The optical properties of a semiconductor are related to both intrinsic and extrinsic effect .PL is a suitable technique to determine the crystalline quality and the exciton fine structure. Fig. 5 and show the PL spectrum corresponding to $\lambda_{ex}= 425\text{nm}$ and $\lambda_{ex}= 450\text{nm}$ respectively. Since the band gap of the present SnO₂ nanoparticles is 4.0 eV(309 nm) as determined from the UV/visible absorption spectrum, the two observed luminescence bands($\sim 526\text{nm}$ and 565nm) can not be attributed to the direct recombination of a conduction electron in the Sn 4d band with a hole in the O 2p valence band. Generally, defects such as oxygen vacancies are known to be the most common defects in oxides and usually act as radiative centers in luminescence processes. Broad luminescence bands between 500 and 600 nm can be explained due to defect levels in the band gap of 1D SnO₂ nanostructures at room temperature in agreement with earlier reports⁹⁻¹⁴.

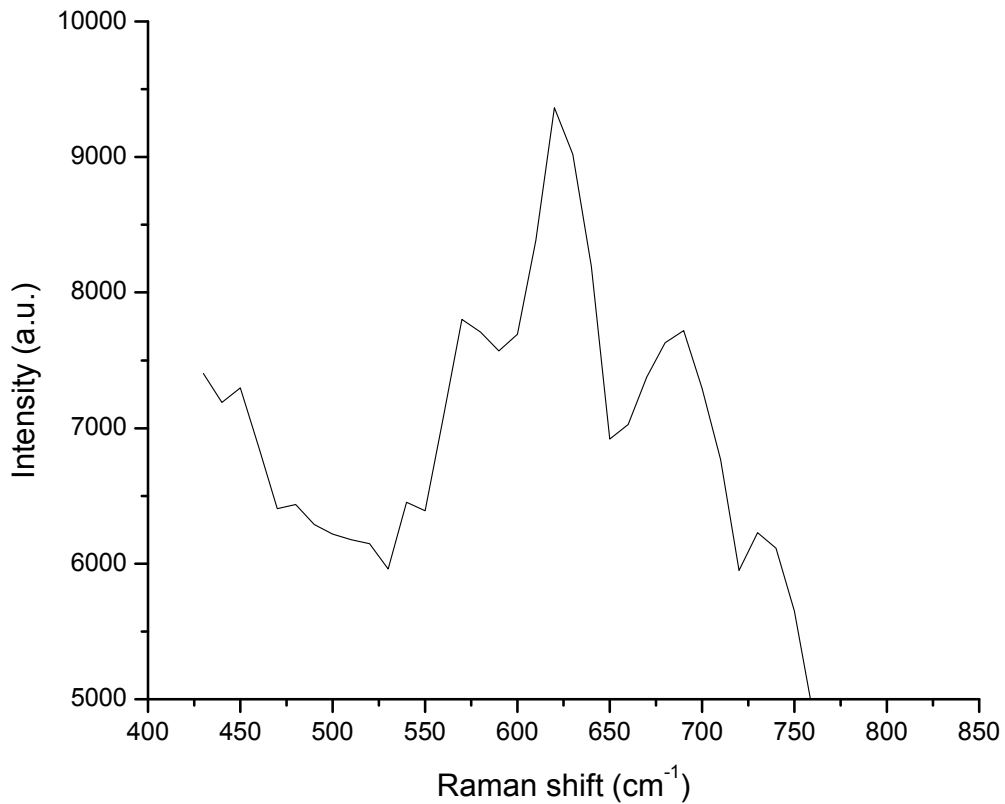


Fig. (6) : Raman spectra of the tin dioxide nanoparticles.

Fig.6 shows the Raman spectrum of the pure tin dioxide nanoparticles. It shows three fundamental Raman peaks at 476, 622 and 731 cm^{-1} , corresponding to the E_g , A_{1g} , and B_{2g} vibration modes of the rutile SnO₂ structure, respectively^{15, 16}. Besides these three main peaks, three abnormal Raman lines are observed at 570, 540, and 690 cm^{-1} corresponding to S_1 , S_2 and S_3 ¹⁶. The S_3 band can be attributed to disorder activation of the acoustic A_{2u} IR active and Raman forbidden mode. Bands S_1 and S_2 arise as a consequence of

reducing particle dimension. The presence of IR modes and forbidden Raman modes can be due to the breaking down of the prevailing $q_0 = 0$ selection rule (where q_0 is the wave vector of the lattice vibration) as the degree of disorder increases (reducing crystal symmetry) or as the crystal size decreases to nanoscale.¹⁷⁻¹⁹

Conclusion : In this paper we have reported the preparation of rutile tetragonal tin dioxide (SnO_2) nanoparticles of average size 7~8 nm by a surfactant mediated method. The crystal structure and the particle size of the sample have been verified by XRD as well as TEM analysis. The band gap of the prepared nanocrystalline SnO_2 have been evaluated with UV-vis Spectroscopy to be 4.0 eV .The absorption spectra shows the blue shift which is attributed to decrease in particle size .The yellow emission bands at 526 nm and 564 nm are attributed to the defect levels in the band gap. The appearance of the three Raman peaks S₁, S₂, and S₃ at 570, 540 and 690nm also support the formation of nanoscale SnO_2 particles.

Acknowledgement : Authors would like to thank Professor Rajen Harshe, Vice Chancellor of University of Allahabad for his motivation and encouragement in carrying the above work. We acknowledge Professor O N Srivastava of Banaras Hindu University for extending TEM facility. Professor R Gopal and Dr A C Pandey are also acknowledged for extending the facilities available with them at laser spectroscopy and nanophosphor application center respectively. One of the authors Ms Jagriti would like to acknowledge UGC for granting a fellowship.

References :

- (1) S.Shukla,S.Patil, S.C. kuiry, Z. Rahman, T.Du, L.Ludwig,C.Parish,S.Seal. Sensors and Actuators B **96** (2003) 343-353.
- (2) Th. Becker,S.Ahlers, Chr.Bosch V Braunmuhl, G. Muller, O.Kiesewetter . Sensors and Actuators B **77** (2001) 55-61.
- (3) A. Heilig, N. Barsan, U. Weimar, M. Schweizer Berberich, J. W. Gardener ,W. Gopel, Sensors and Actuators B **43** (1997) 45-51.
- (4) Kohl D. J.Phys D: Appl. Phys 2001, 34 R125.
- (5) Yu-de Wang, Chun-Lai Ma, Xiao-dan Sun, Heng-de Li, Nonotechnology 13(2002) 565-569.
- (6) Hyoun Woo Kim, Seung Hyun Shim, Ju Hyun Myung. Brazilain Journal of Physics , vol. 35 no. 4A,December 2005.
- (7) Min-Sik Park, Guo- Xiu Wang, Yong-Mook Kang, David Wexler, Shi-Xue Dou, Hua- Kun-Liu. Angew. Chem. Int. Ed. 2007, 46, 750-753.
- (8) Feng Gu, Shu Wang, Meng Kai Lu, Guang Jun Zhou, Dhong Xu, Duo Rong Yuan J. Phys.Chem. B 2004, 108, 8119-8123
- (9) Hu J Q, Ma X L, Shang N G, Xie Z Y, Wong N B, Lee C S, Lee S T 2002 J. Phys. Chem.B **106** 3823.
- (10) Hu J Q, Bando Y, Liu Q L , Golberg D 2003 Adv. Funct. Mater. **13** 493.
- (11) Calestani D, Lazzarini L, Salviati G , Zha M 2005 Cryst. Res. Technol. **40** 937.
- (12) Fagila G , Baratto C , Sberveglieri G, Zha M , Zappettini A 2005 Appl. Phys. Lett. **86** 011923.
- (13) Cai D, Su Y , Chen Y , Jiang J, He Z , Chen L 2005 Mater. Lett. **59** 1984.

- (14) Maestre D; Cremades A , Piqueras. J 2005 J. Appl. Phys. **97** 044316.
- (15) Peercy, P.S.; Morosin, B. Phys. Rev. B 1973, 7 , 2779-2786.
- (16) A.Dieguez; A. Romano-Rodriguez; A. Vila , J.R. Morante. J. Appl. Phys. Vol. 90, No. 3 , 1 August 2001.
- (17) Peng, X. S.; Zhang, L. D.; Meng, G. W.; Tian, Y. T.; Lin, Y.; Geng, B.Y.; Sun, S.H. J. Appl. Phys. 2003, 93, 1760-1763.
- (18) Zhou, J.X.; Zhang, M. S.; Hong, J. M.; Yin, Z. Solid State Commun. 2006, 138, 242-246.
- (19) Wang, J. X.; Liu, D. F.; Yuan, H. J.; Ci, L. J.;Zhou, Z.P.; Gao, Y.; Song, L.; Liu, L. F.; Zhou, W. Y.; Wang, G.; Xie, S. S. Solid State Commun. 2004, 130, 89-94.